INTERNATIONAL SOCIETY FOR
SOIL MECHANICS AND
GEOTECHNICAL ENGINEERING

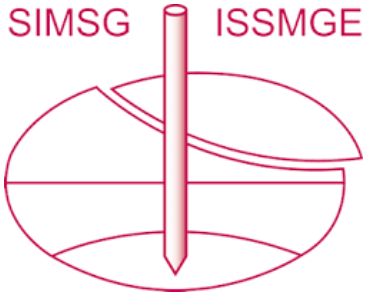

This paper was downloaded from the Online Library of the International Society for Soil Mechanics and Geotechnical Engineering (ISSMGE). The library is available here:

https://www.issmge.org/publications/online-library

This is an open-access database that archives thousands of papers published under the Auspices of the ISSMGE and maintained by the Innovation and Development Committee of ISSMGE.

5ICEGE
5th International Conference on Earthquake Geotechnical Engineering
January 2011, 10-13 | Santiago, Chile
Paper No. NONAS

A NONLINEAR MACROELEMENT FOR DYNAMIC SOIL-STRUCTURE INTERACTION ANALYSES OF PILE FOUNDATIONS IN LIQUEFIABLE SOILS

VARUN [1], Dominic ASSIMAKI[2]

ABSTRACT

We here present a macroelement for soil-structure interaction analyses of piles in liquefiable soils, which captures efficiently the fundamental mechanisms of saturated granular soil behavior. The mechanical model comprises a nonlinear Winkler-type model that accounts for drag forces in the circumference of the pile and soil-pile interface nonlinearities, and a coupled viscous damper that simulates changes in radiation damping with increasing material and interface non-linearity. 3D FE simulations are conducted for a pile in radially homogeneous soil to identify the critical parameters governing the response. Dimensional analyses are next conducted, and the importance of hydraulic conductivity and loading rate of dynamic loading in saturated soils is emphasized. Next, the macroelement parameters are calibrated as a function of the soil properties and the effective stress. A semi-empirical approach is used to generate pore pressure histories and detect the onset of liquefaction in absence of the structure. By adjusting the apparent permeability of the soil surrounding the pile, the model can be also used to estimate the effectiveness of measures against liquefaction such as vertical drains or grouting as part of structural risk assessment studies. The macroelement is finally implemented in a finite element code, and the estimated response of structural members is benchmarked by comparison with fully coupled 3D FE analyses, field tests and centrifuge experiments.

Keywords: piles, soil liquefaction, soil-structure interaction, 3D finite elements

INTRODUCTION

Pile foundations are used quite extensively to support variety of structures especially those built on loose/soft soils. Other than vertical loads, pile foundations are often subjected to lateral loads during seismic events. Soil-structure-interaction plays an important role in evaluating the response of pile foundations to lateral loads (Mylonakis and Gazetas [1]). Various methods for analyzing seismic soil-structure interaction include finite-element or finite-difference methods and dynamic beam on non-linear Winkler foundation (BNWF) method. BNWF method, also referred to as 'p-y' approach, assumes that each layer of soil responds independently of adjacent layers of soil and hence can be replaced by a discrete spring. Backbone p-y curves for monotonic loading have been recommended by Matlock [2], Reese et al. [3] and API [4]. For pile response in liquefiable soils, the load-displacement curves for non-liquefiable soils are scaled by reduction factors (referred to as p-y multipliers) as a function of the pore-pressure ratio in the soil to account for the soil strength reduction during liquefaction. p-y multipliers have been suggested by Japan Road Association [5], the Architectural Institute of Japan [6], Liu & Dobry [7], Wilson et al [8] and Brandenberg et al. [9].

[1] Research Assistant, CEE, Georgia Tech, e-mail: varun.rai@gmail.com
[2] Assistant Professor, CEE, Georgia Tech, e-mail: dominic.assimaki@ce.gatech.edu

While these empirical factors have been developed based on liquefaction experimental data, the monotonic stress-strain response predicted is qualitatively similar to the response of non-liquefiable soils, namely reflects strain-softening behavior. By contrast, field experimental data obtained during blast induced liquefaction testing at Treasure Island by Weaver et al. [10], as well as large scale shake table tests by Tokimatsu et al. [11], show that the macroscopic response of piles in liquefiable soils should be qualitatively described by a strain-hardening model. Furthermore, this approach also does not account for rate-dependent response due to radiation damping and seepage effects (Yoshimine [12]). Bridging the gap between empirical models and sophisticated numerical simulations, we here develop a macroelement for soil-structure interaction analyses of piles in liquefiable soils, which captures macroscopically the fundamental mechanisms of saturated granular soil behavior.

DYNAMIC SOIL-PILE INTERACTION SIMULATIONS

Numerical Framework

Due to the limited number of experimental data, the macroelement components were developed based on 3D FE simulations, yet validated by comparison with available large and small-scale experiments. Parametric analyses were conducted using the finite element code DYNAFLOW (Prevost [13]) for a single pile in homogeneous liquefiable soil. A uniform displacement was imposed along the length of the pile to replicate the response of a slice of the full 3D numerical domain perpendicular to the cross section of the pile. Both soil and pile were modeled as porous solids using four node quadrilateral elements. The pile is simulated as an elastic material with very low permeability to avoid coupling of structural non-linearity with the soil response. The soil is simulated by means of a pressure dependent multi-yield plasticity model with associative flow rule for the deviatoric (distortional) component and a non-associative flow rule for the volumetric component (Prevost [14]). Dynamic soil-fluid coupling in the soil material was achieved via the extension of Biot's theory as shown by Prevost [15]. The parameters for the constitutive soil model used in this study are presented in **Table 1**.

Table 1. Material parameters for the soil model.

Property	Symbol	Range	Property	Symbol	Range
Elastic Parameters			**Yield Parameters**		
Shear Modulus	G_s	2 MPa	Peak Friction Angle	φ	32-38°
Bulk Modulus	K_s	4 MPa	Max. shear strain	γ_{max}	0.04-0.08
Power Exponent	n	0.5-0.7	**State Parameters**		
Dilation Parameters			Porosity	n^w	0.2-0.4
Critical state Friction angle	φ_{ss}	22-30°	Hydraulic conductivity	k	10^{-3}-10^{-6} m/s
Liquefaction Strength	χ	0.0-0.15	Solid phase density	ρ_s	2650 kg/m^3

Non-linear iterations were performed using the Quasi-Newton technique with BFGS update formula. Time integration was performed using the Newmark method with γ=0.65 and β=0.33 to reduce any high frequency noise. Taking advantage of symmetry in both geometry and loading of the problem, only half of the domain was simulated to reduce computational time. In the simulated numerical domain, the far-field lateral boundary is defined 10 pile diameters away from the pile centerline. At the lateral boundary, both the solid and liquid phases are constrained from moving in the radial direction. In the first phase of simulation, gravity is applied as a body force and the soil is allowed to consolidate under its own weight leading to the development of depth-dependent effective stress and hydrostatic pore pressure in geostatic equilibrium. In the second phase, prescribed displacements are imposed on center nodes of pile along the entire length and reactions are recorded.

Parametric Analyses

The numerical results compared very well with a series of important observations made in centrifuge tests, and offered additional insight in mechanisms manifesting due to soil-structure interaction in liquefiable sites. The observations are summed up below. For details the reader is referred to Varun [16]:

(a) Initially, the p-y curves show strain-softening behavior with stiffness decreasing as displacement increases. Since, the soil has a tendency to contract for stress ratios τ/σ' below the phase transition line, the initial cycles of cyclic loading lead to accumulation of excess pore pressure and the response degrades with increasing number of cycles. However, after the effective stress in the vicinity of the pile reaches a lower-bound threshold, phase transformation is observed in the soil and strain-hardening response results from the dilating tendency of soil.

(b) After a certain number of cycles, the pile response reaches a steady-state condition where the rate of increase in pore-pressures equals the rate of dissipation causing the average soil effective stress in the immediate vicinity of the pile during a cycle of loading to remain constant. While the rate of pore pressure buildup is a function of the amplitude and frequency of loading, the pore-pressure dissipation is partially achieved via radial flow away from the pile, and is controlled by hydraulic conductivity of soil. This was verified by the fact that the same response was observed by keeping the ratio of permeability and frequency the same for very low frequencies, for which the effects of radiation damping are insignificant. For high hydraulic conductivity ($k=10^{-3}$ m/s), the rate of drainage of excess pore pressure is faster than rate of generation and hence the response shows almost no degradation; as hydraulic conductivity decreases, pore pressure generation starts dominating with the response for $k=10^{-5}$ m/s being almost the same as the completely undrained response.

(c) It is observed that the steady-state response depends on the dilation angle (δ) as well. Soils with higher dilation angle retain higher percentage of their original strength at lower permeability compared to others. This observation agrees well with those from centrifuge tests by Wilson at el. [8] where medium-dense sands were found to retain higher (25-30%) of their original strength compared to loose sands (10%) during liquefaction.

(d) For same value of liquefaction resistance parameter, the soil at lower depth liquefies earlier as compared to soil at higher depths. For low displacement levels, the soil resistance is attributed primarily to the drag force exerted by the liquefying soil flowing around the pile and is observed to be almost constant at $p \approx 10$ kN/m, irrespective of the depth. Given the pile diameter of B=1m in the model, this observation matches very well with a depth independent constant lateral pressure of 10.3 kPa recommended by Abdoun et al. [17] and Dobry et al. [18] for liquefied sands. However, once phase transformation takes place in the soil surrounding the pile, the residual resistance increases with increasing depth.

(e) The effect of liquefaction resistance of the soil directly translates to the liquefaction resistance of the macroscopic pile response, i.e., pile response in soils with higher liquefaction degrades at slower rate.

(f) The load at which phase transition is observed is directly proportional to effective stress in vicinity of the pile (S). The slope of this phase transition line is independent of amplitude of loading; and the rate at which the effective stress ratio (S) decreases with each loading cycle is different for different loading amplitudes, however after the soil in vicinity of the pile has undergone phase transition into the dilative zone, further shearing doesn't contribute much to accumulation of excess pore pressures.

(g) As the loading frequency increases, the amount of energy dissipated, i.e., the area enclosed by the loop also increases. This is expected since radiation damping increases with loading rate. Also, there are no clearly demarcated regions of unloading-reloading since the stiffness and damping response are 90 degrees out of phase. While one is decreasing (unloading), the other one is increasing (loading) and vice-versa.

MACROELEMENT FORMULATION

Results of the parametric investigation suggest that the total resistance as seen from the pile centerline is a function of the effective stress distribution around the pile, which in turn is a function of permeability of the soil and the frequency of loading. Based on this observation, we propose a macroscopic constitutive model to capture pile response in dry soil. We next modify the response by means of a pore pressure generator to account for the response in drained and partially drained conditions.

Drained / Dry Loading

To model the response of a pile subjected to lateral loading in dry / drained soil conditions, a modified Bouc-Wen type hysteresis model (Bouc [19]; Wen [20]) is used. Similar models have been implemented in the past by Badoni & Makris [21] for modeling seismic response of pile foundations. The governing equation for the quasi-static case is given as:

$$p = p_y \zeta \tag{1}$$

where p_y is the ultimate lateral resistance and ζ is a hysteretic dimensionless quantity controlling the nonlinear behavior of the lateral soil reaction. A dashpot is added to the model to simulate radiation damping caused by energy dissipation and redistribution effects. The dashpot can either be placed in "parallel" or "series" with the spring. However, Wang et al. [22] showed that parallel arrangement can result in excessive forces when loaded in highly non-linear range unless an upper bound is ensured for this case. Based on results from parametric analyses and above mentioned criteria, a formulation similar to "series" arrangement is used in our model implemented as follows:

The total resistance is thus calculated in an incremental fashion as

$$dp = dp_s + dp_d = p_y d\zeta_s + p_y d\zeta_d \tag{2}$$

$$d\zeta_s = \left\{1 - f_\zeta \left[b + g\,\text{sign}(du.\zeta)\right]\right\} \frac{du}{u_y} \tag{3}$$

where $u_y = p_y / K$ is the yield displacement, K is the initial stiffness, du is the incremental relative displacement between the pile and the free-field at the location of macroelement, $b = 1 - g$ are parameters controlling unloading and reloading stiffness, $sign(x) = -1$ if x < 0 and +1 if x ≥ 0 is the sign function, and f_ζ is a monotonically increasing function of ζ such that $f(\zeta) = 1$ when $\zeta = 1$ and $f(\zeta) = 0$ when $\zeta = 0$.

$$dp_d = c_r d\dot{u} \tag{4}$$

where c_r is the radiation damping coefficient; to account for the soil nonlinearity effects on radiation damping, c_r is approximated iteratively using an equivalent linear approach (i.e. using the tangent modulus of the stress-strain hysteresis loop instead of the elastic stiffness) by modifying the linear damping coefficient by Makris and Gazetas [23] as follows:

$$\begin{aligned} c_r &= c\left[1 - f_\zeta\left(b + g\,\text{sign}(du.\zeta)\right)\right]^{0.5} \\ c &= \rho_s V_s a_o^{-0.25} QB \end{aligned} \tag{5}$$

where ρ_s is the density of soil, V_s is the shear wave velocity in soil, B is pile diameter, $a_o = \omega B / V_s$ is the normalized frequency of loading, and Q is a shape factor that depends on the soil Poisson's ratio but can be approximately set to $Q \approx 3$ for shallow depths (Badoni & Makris [21]). In case of transient loading, ω is set equal to the dominant frequency of loading. The non-linear formulation ensures that when $\zeta = 1$, $c_r = 0$ and hence the total force never exceeds the ultimate resistance of soil.

Undrained Loading

We next integrate the effects of effective stress changes on the soil-pile response. The average effective stress in the vicinity of the pile is evaluated by using the 'liquefaction front' concept developed by Iai et al. [24] and extending it for the case of piles. This approximation is based on the observation that the pore pressure generation is directly proportional to the total amount of plastic shear work done per unit volume of soil (Towhata and Ishihara [25]). The response is written in terms of two dimensionless parameters, the average effective stress $S = \sigma_v' / \sigma_{v0}'$ that can be written in terms of normalized soil resistance $r = p / B\sigma_i'$ as follows:

$$S = \begin{cases} S_o & (r \le r_3) \\ S_2 + \sqrt{\left(S_o - S_2\right)^2 + [(r - r_3)/m_1]^2} & (r > r_3) \end{cases} \tag{6}$$

where $S_2 = S_0\left(1 - m_2/3m_1\right)$, $r_3 = 2S_0 m_2/3m_1$, m_1 is the slope of failure line and m_2 is the slope of phase transformation line. S_0 is defined in terms of normalized plastic shear work (w), shear work normalization parameter (w_1) and parameter controlling the shape of strength degradation curve (κ) and is calculated incrementally as follows:

$$S_0 = \exp\left(\frac{w}{w_1}\right)^{\kappa} \tag{7}$$

$$dS_0 = \kappa S_0 (-\log S_0)^{(\kappa-1)/\kappa} dw / w_1 \tag{8}$$

The quantity dw is the normalized incremental plastic shear work, and is calculated as the difference between total incremental shear work and elastic incremental shear work normalized by the product of ultimate soil resistance and yield displacement (see Equation (9)). Since the results from our parametric investigation on cyclic displacement amplitude indicate that the amount of plastic shear work done when the soil is in "dilation" doesn't contribute significantly to the build-up of excess pore pressure, only the plastic shear work done in "contractive" zone is used as follows:

$$dw = \begin{cases} \dfrac{dW - dW_e}{p_y u_y} = \dfrac{p.du - p.(dp/K)}{p_y u_y} & r \le r_3 \\ 0 & r > r_3 \end{cases} \tag{9}$$

According to Iai et al [32], a drawback of the formulation in equation (6) is that it becomes unstable when the r-S curve approaches the failure line; for the macroelement, this implies that when $\zeta = 1$, $S/S_0 \to \infty$. To avoid this problem and improve the response idealization obtained in parametric analysis, we impose the condition that the failure slope m_1 be increased by a factor of $1.05 + 0.4S_0$. In this way, the increment of 0.05 of the intercept bounds the total response and avoids numerical instability at $\zeta = 1$, while the $0.4S_0$ term prevents overestimation of dilation response when the soil in the vicinity of pile is not liquefied.

Partially Drained Loading

Gonzalez et al. [26] among others reported that the interaction between pile and soil during liquefaction leads to the formation of a zone around the pile where pore pressures are considerably different from those in the far-field. This difference has been attributed to both dilation effects in the soil as well as suction on the 'tension' side of pile. Similar phenomenon was observed in our numerical analyses, where the liquefaction caused by the relative soil-pile motion was confined within a zone of about five diameters around the pile.To account for the effects of partial drainage, it is assumed that there is a linear pressure

gradient between the near-field and the far-field in the radial direction, and that Darcy's Law may be applied. The change in S_0 parameter due to drainage is written as:

$$V = k\frac{\Delta h}{L} = \frac{k}{L}\sigma'_{v0}\left(S_{ff} - S\right) \propto \frac{d\varepsilon_v}{dt} = \frac{dS_0}{dt}\frac{\sigma'_{v0}}{K_s} \tag{10}$$

where k is the permeability of soil, S_{ff} is the effective stress ratio in free-field, ε_v is the volumetric strain released due to outflow of water, K_s is the bulk modulus of soil and the drainage length $L \propto B$. Since $K_s \propto S^n$, the expression above can be modified and written in implicit form as:

$$dS_0 = \frac{\beta.dtS^n}{1+\beta.dtS^n}\left(S_{ff} - S\right) \tag{11}$$

where $\beta = f\left(k/B\right)$.

Gap Element

In order to simulate the effect of gapping, a gap formulation is used which essentially is an envelope function used to scale the total p-y response predicted by the macroelement depending on the current displacement and the maximum previous displacement on each side of the pile. The following function is used and the gap multiplier is calculated as

$$m_g = c_d + \left(1 - c_d\right)\frac{u_{ref}^2}{u_{ref}^2 + \left|u - u_{\max}\right|^2} \tag{12}$$

Where c_d is the ratio of drag resistance from sides to total resistance and is typically equal to 0.1, $u_{\max}$ is the maximum previous displacement on each side and u_{ref} is a reference displacement value used for scaling. The reference displacement is chosen as $u_{ref} = 5u_y$ where $u_y = p_y / K$ is the yield displacement and u_{ref} roughly corresponds to the displacement at which 50% of maximum resistance is mobilized.

Calibration

The macroelement is next calibrated based on 3D FEM simulations where the model parameters are related to soil parameters as shown below. For a detailed description of calibration procedure the reader is referred to Varun & Assimaki [27].

(a) The initial stiffness of model

$$K = 1.25E_s \tag{13}$$

(b) Yield strength or ultimate soil resistance per unit length

$$p_y = \left(3.25K_p + 0.3K_p^2\right)B\sigma_v' \tag{14}$$

Where $K_p = \tan^2\left(45 + \varphi/2\right)$ is the coefficient of passive earth pressure

(c) Backbone curve

A backbone function of $f_\zeta = \tanh\left(\alpha|\zeta|\right)/\tanh\left(\alpha\right)$ is used. A value of α =2.7 for dense sands, 2.8 for medium-dense and 2.9 for loose sands is recommended.

(d) Unloading-Reloading stiffness parameters

b = 0.6 and g = 0.4

(e) Slope of phase transition line

$$m_2 = 3.25\tan^2\left(45^\circ + \varphi_{ss}/2\right) \tag{15}$$

(f) Shear work correlation parameter

$$w_1 = n^{(1-n)}(1-2\nu)^{2n}(1-\nu)^{2(1-n)} / \chi \quad (16)$$

(g) Drainage parameter

$$\beta = 550\frac{2(1+\nu)}{3(1-2\nu)}\frac{k}{B} \quad (17)$$

VALIDATION

The performance of macroelement is validated next by comparison with two different kinds of tests. The first type consists of field tests where liquefaction is induced by means of controlled blasting followed by lateral loading of pile. The second type consists of centrifuge experiments where the pile with a superstructure is excited by means of seismic loading.

Comparison with Field Test using Blast Induced Liquefaction

The field test was conducted at National Geotechnical Experimentation site at Treasure Island, California. The site consists of loose sands underlain by young bay mud. The site conditions are presented in detail along with corrected blow counts (SPT), Cone Tip Resistance (CPT), Relative density and friction angle by Weaver et al. [10].

The critical state friction angle (φ_{ss}) is estimated using the relative density and friction angle (φ). For very loose sands (D_r = 20%, $\varphi - \varphi_{ss} = 1 - 2^\circ$) whereas for loose sands (D_r = 50%, $\varphi - \varphi_{ss} = 3^\circ$) is used. The liquefaction resistance parameter is estimated from SPT blowcounts as recommended by Popescu and Prevost [28]. Finally the drainage parameter (β) is estimated directly from the dissipation rate of excess pore pressure right next to pile. A value of β = 0.0021 (1/s) is obtained which corresponds to k = $6.7\text{x}10^{-6}$ m/s which seems a reasonable value for medium to fine sands. A total of 16 macroelements were used along the length of pile. Using the soil parameters, the macroelement parameters were estimated using the relationships described in previous section and are described in detail in Varun [16]. The parameter S_{oi} is the initial value of effective stress ratio, i.e., $1 - r_u$ in the near field just after blasting and is determined directly from the pore pressure histories.

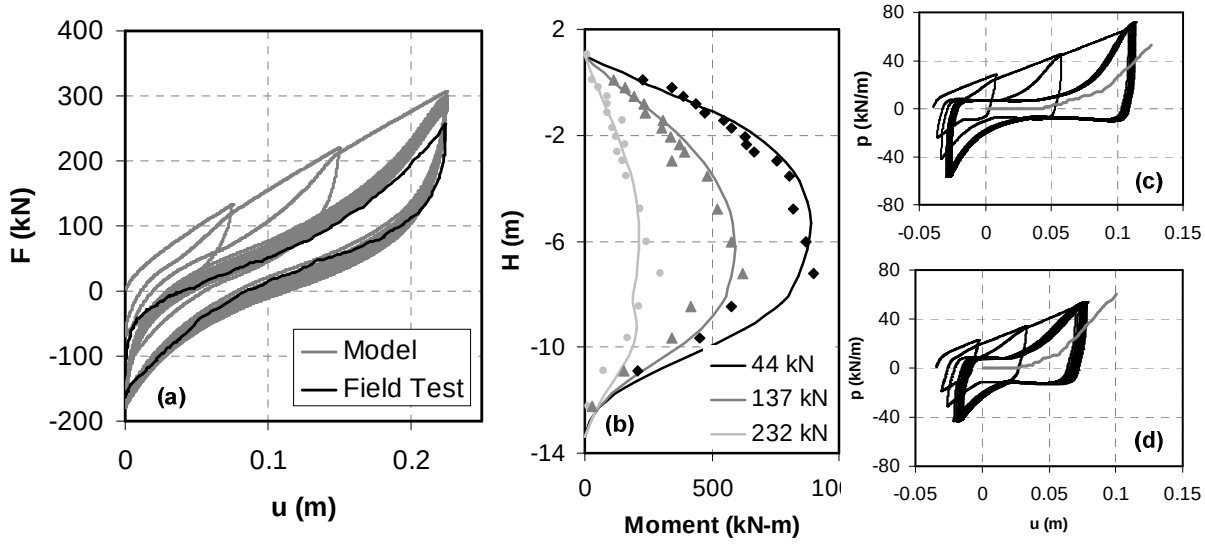

Figure 1 Comparison between (a) observed and predicted lateral force at pile top (b) Bending moments at three different load levels (c) simulated behavior vs back calculated p-y backbone at 1.5 m depth and (d) 3.0 m depth

The pile has a diameter of 0.6 m and EI = 291,800 kN/m^2. After blasting, the loading was applied in half loading cycles using a swivel head to provide free head condition. The first series of loading consisted of one 75 mm, one 150 mm followed by eleven 225 mm displacement cycles at a rate of 10 mm/min. Due to slow loading rate, the radiation damping was considered to be negligible in the model. Figure 1 (a) shows the total force recorded at pile head vs. displacement. The observed values for last loading cycle during field test are also shown. Very good agreement is obtained between the observed and predicted values. Good agreements between bending moment are also observed as shown in Figure 1(b). The simulated p-y curves recorded at depths of 1.5 m and 3.0 m also agree well with back calculated p-y backbone as seen in Figure 1(c) and (d), respectively.

Comparison with Centrifuge Tests

The centrifuge tests were conducted at National Geotechnical Centrifuge at UC Davis with an acceleration of 30g. A mixture of water and methyl cellulose with a viscosity 10 times that of water was used as the pore fluid. Two particular configurations referred to as CSP_2 and CSP_3 are chosen for simulation. CSP_2 consists of 9 m thick layer loose Nevada sand on the top (D_r = 35-40%) underlain by Dense Nevada sand (D_r = 80%) whereas the upper layer in CSP_3 is medium dense Nevada sand (D_r = 55%). Nevada Sand is fine, uniform sand (C_u =1.5, D_{50} = 0.15 mm) and its behavior has been extensively studied in both laboratory and centrifuge tests during the VELACS project (Arulanandan and Scott [29]). Hence the soil properties are reasonably well documented (Popescu and Prevost [28]) and are shown in Table 2. Using the soil properties, the macroelement properties are calculated as described in detail in Varun [16]. Both the models are subjected to two events A and B that are scaled versions Kobe 1995 earthquake. Event A has a maximum acceleration of 0.04 g whereas event B has a maximum acceleration of 0.22g. For the purpose of comparison, the highly instrumented single pile was used for both models. The pile had a Young's modulus (E_p) = 70 GPa and Area moment of Intertia (I) = 0.0061 m^4. The superstructure mass (M_{ss}) was 49140 kg. The input displacement histories for free-field end of macroelement were obtained by integrating the acceleration time histories recorded in free field in the centrifuge at seven locations and using linear interpolation for the other seven. The excess pore pressure ratio time histories were also obtained from pore pressure transducers in centrifuge experiments themselves.

Table 2. Soil Properties for Centrifuge Tests

Property	Unit	Dr = 35%	Dr = 55%	Dr = 80%
Shear Modulus (Go)	MPa	25	30	40
Bulk Modulus (Ko)	MPa	50	55	100
Power Exponent (n)	--	0.7	0.7	0.7
Friction angle (φ)	Degrees	32	34	38
CS Friction angle (φ_{ss})	Degrees	30	30	30
Liquefaction (χ)	--	0.16	0.14	0.06
Permeability (k)	m/s	$6.6\text{x}10^{-5}$	$5.6\text{x}10^{-5}$	$4.7\text{x}10^{-5}$

Model CSP_2

Figure 2(a)-(c) shows the acceleration time histories at the Pile Head, and acceleration and displacement time histories at the Superstructure, respectively for both recorded and predicted cases for event A whereas Figure 2(d)-(f) shows the same for event B. It can be seen that all the time histories are in good agreement with each other for both the events. Figure 5(a) and (b) show the observed and predicted maximum moment profiles for events A and B, respectively. The bending moments are predicted quite well within 25% accuracy. Finally, Figure 3 shows the p-y response for three macroelements for event A and Figure 4 for event B. While event A doesn't mobilize the soil resistance lower than 2.0 m and the soil response below that is almost linear, significant non-linearity can be seen all the way up to 3.5 m for event B.

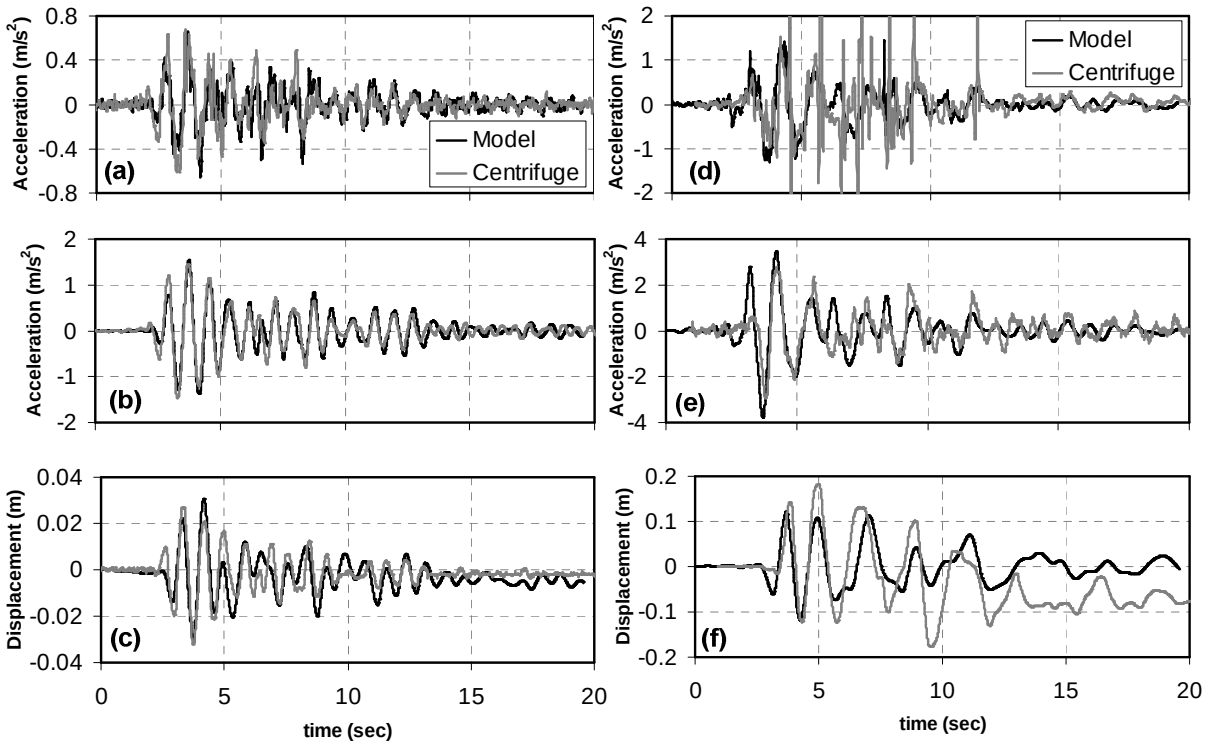

Figure 2 Time histories of (a) pile head acceleration (b) superstructure acceleration (c) superstructure displacement for event A and (d)-(f) for event B for profile CSP_2.

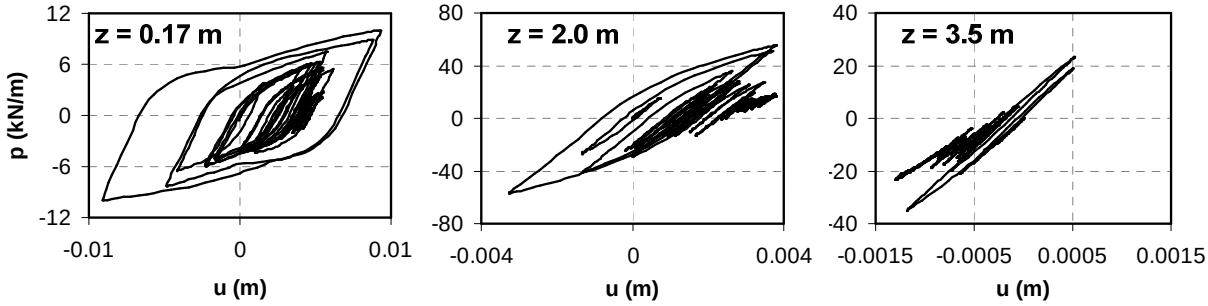

Figure 3 Dynamic p-y response at three different depths for CSP_2 event A

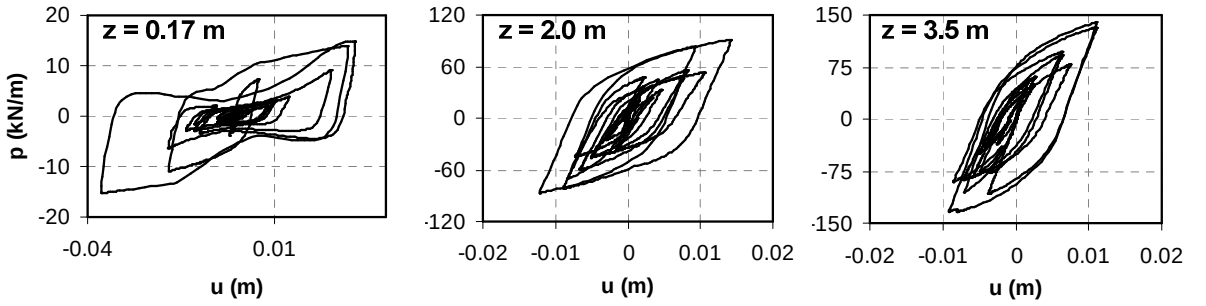

Figure 4 Dynamic p-y response at three different depths for CSP_2 event B.

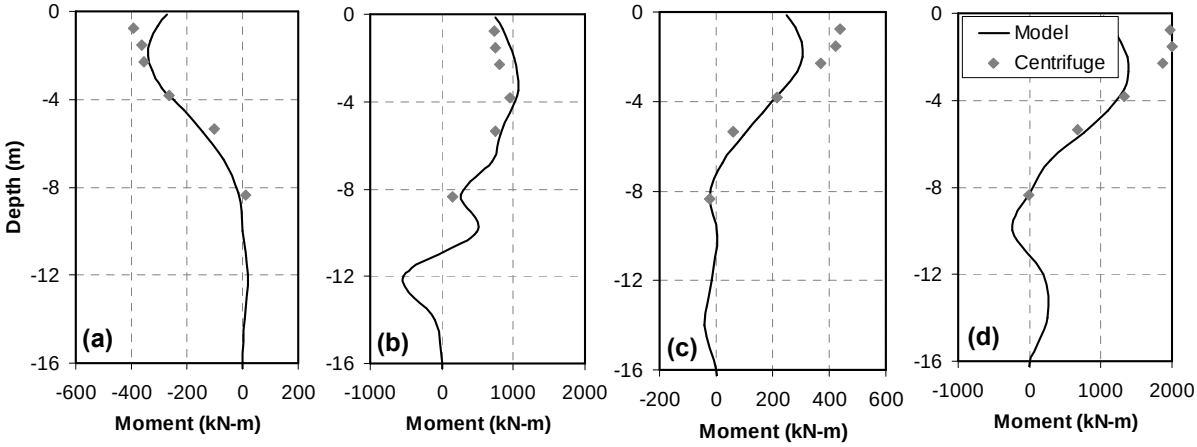

Figure 5 Predicted vs. Observed Peak bending moments with depth for (a) CSP_2 event A (b) CSP_2 event B (c) CSP_3 event A (d) CSP_3 event B.

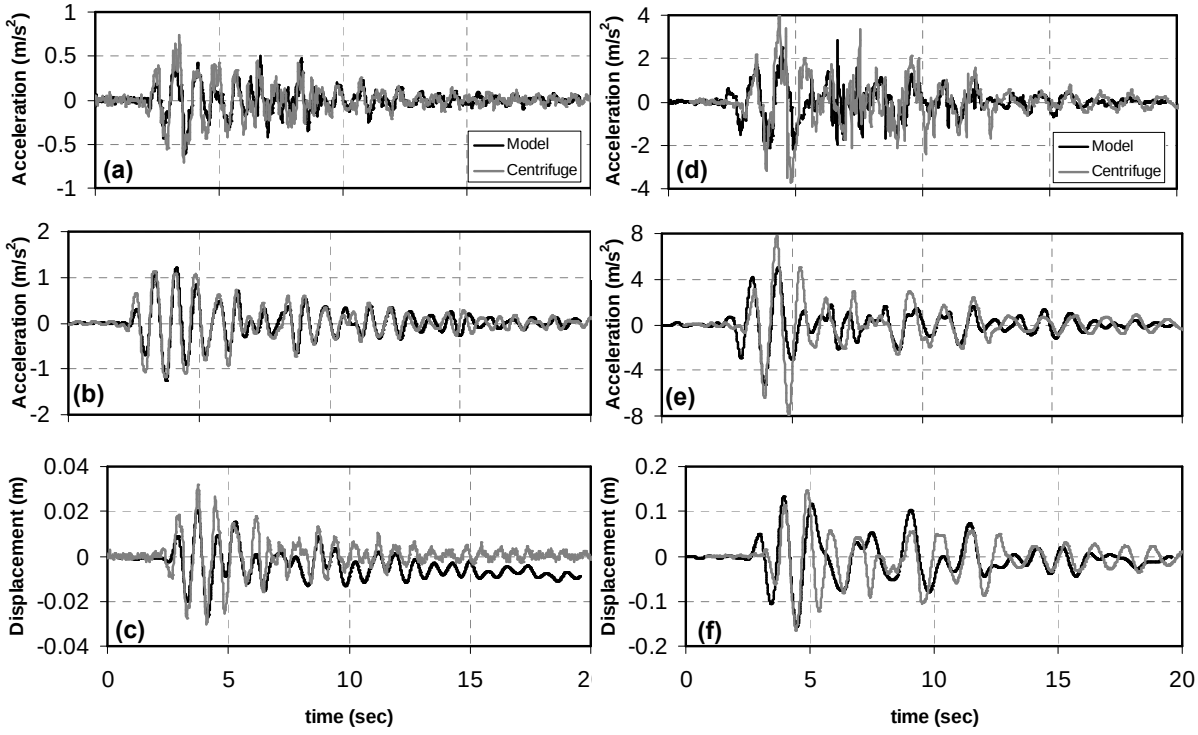

Figure 6 Time histories of (a) pile head acceleration (b) superstructure acceleration (c) superstructure displacement for event A and (d)-(f) for event B for profile CSP_3.

Model CSP_3

Figure 6(a)-(c) shows the acceleration time histories for event A whereas Figure 6(d)-(f) shows the same for event B. The time histories are in good agreement for event A, but for event B the numerical model predicts lower peak accelerations (2.5 m/s^2 predicted vs. 4.0 m/s^2 observed at pile head and 5.0 m/s^2

predicted vs. 8.0 m/s^2 observed at superstructure). Similar trend is observed in bending moments in top 2 m for both event A and B as shown in Figure 5 (c) and (d), respectively. The bending moments are predicted quite well below 2 m but are around 25% lower for top 2 m. When comparing the response with back calculated p-y curves presented in Wilson [30], it was observed that the back calculated p-y curves from centrifuge experiment at 1.2 m depth show a very stiff response (even stiffer than the response for drained conditions) probably due to excessive drag force which arises due to higher viscosity of pore fluid due to scaling. The stiffer response of soil in top 1.2 m compared to actual response if there were no scaling issues explains the lower predicted moments in top 2 m and also lower predicted accelerations.

CONCLUSIONS

We presented a detailed parametric investigation of the dynamic response of single piles in liquefiable soils using 3D FEM simulations. The numerical results compared very well with a series of important observations made in centrifuge tests, and offered additional insight in mechanisms manifesting due to soil-structure interaction in liquefiable sites. Based on the numerical results, we then proposed a generic macroelement that can be used to simulate the observed pile response parameterized as a function of the soil properties that were identified from the parametric investigation. The calibration of these parameters is performed using 3D FEM simulations. The validation and benchmarking was performed next by comparison with field data from blast induced liquefaction tests, and seismic soil structure interaction data from centrifuge test. The macroelement was shown to perform well in both situations, namely when: (a) direct loading is applied to the structure and structural loading is the primary source of excess pore pressure generation (field tests) and (b) both loading and excess pore pressure comes primarily from far-field initially followed by inertial loading from the superstructure (centrifuge tests).

ACKNOWLEDGEMENTS

This material is based upon the work supported by the National Science Foundation under Grant Nos. CMS-0530478 and CMS-0402490. Any opinions expressed in this material are those of the author(s) and do not necessarily reflect the views of NSF.

REFERENCES

[1] G. Mylonakis, G. Gazetas, Seismic soil-structure interaction: Beneficial or detrimental?, J Earthquake Eng, 4 (2000) 277-301.
[2] H. Matlock, Correlations for design of laterally loaded piles in soft clay, in: 2nd Annual Offshore Technology Conference, 1970, pp. 577-594.
[3] L.C. Reese, W.R. Cox, F.D. Koop, Analysis of laterally loaded piles in sand, in: Offshore Technology Conference, 1974, pp. 473-484.
[4] American Petroleum Institute, Recommended Practice for Planning, Designing and Constructing Fixed Offshore Platforms, in: API Recommended Practice 2A, Washington, D.C., 1993.
[5] Japan Road Association, Specifications for highway bridges, in: Part V, Seismic Design, Japan, 1996.
[6] Architectural Institute of Japan, Recommendations for design of building foundations, in, Tokyo, 2001.
[7] L. Liu, R. Dobry, Effect of liquefaction on lateral response of piles by centrifuge model tests, National Center for Earthquake Engineering Research (NCEER) Bulletin, 9 (1995) 7-11.
[8] D.W. Wilson, R.W. Boulanger, B.L. Kutter, Observed seismic lateral resistance of liquefying sand, J Geotech Geoenviron, 126 (2000) 898-906.

[9] S.J. Brandenberg, R.W. Boulanger, B.L. Kutter, D. Chang, Static pushover analyses of pile groups in liquefied and laterally spreading ground in centrifuge tests, J Geotech Geoenviron, 133 (2007) 1055-1066.
[10] T.J. Weaver, S.A. Ashford, K.M. Rollins, Response of 0.6 m cast-in-steel-shell pile in liquefied soil under lateral loading, J Geotech Geoenviron, 131 (2005) 94-102.
[11] K. Tokimatsu, H. Suzuki, Y. Suzuki, Back-calculated p-y relation of liquefied soils from large shaking table tests, in: S. Prakash (Ed.) Fourth International Conference on Recent Advances in Geotechnical Earthquake Engineering and Soil Dynamics, 2001, pp. 6-24.
[12] M. Yoshimine, Liquefied soil-pile interaction and its rate effects, in: First Japan-US workshop on Testing,Modeling and Simulation in Geomechanics, Boston, 2003.
[13] J.H. Prevost, DYNAFLOW: A nonlinear transient finite element analysis program, in, Dept. of Civil Engineering and Operations Research, Princeton University, Princeton, NJ, 1995.
[14] J.H. Prevost, A Simple Plasticity Theory for Cohesionless Frictional Soils, International Journal of Soil Dynamics and Earthquake Engineering, 4 (1985) 9-17.
[15] J.H. Prevost, Wave Propagation in Fluid-Saturated Porous Media: An Efficient Finite Element Procedure, International Journal of Soil Dynamics and Earthquake Engineering, 4 (1985) 183-202.
[16] Varun, A Non-Linear Dynamic Macroelement for Soil Structure Interaction Analyses in Liquefiable Soils, PhD Dissertation, in: Civil and Environmental Engineering, Georgia Institute of Technology, Atlanta, 2010.
[17] T. Abdoun, R. Dobry, T.D. O'Rourke, S.H. Goh, Pile response to lateral spreads: Centrifuge modeling, J Geotech Geoenviron, 129 (2003) 869-878.
[18] R. Dobry, T. Abdoun, T.D. O'Rourke, S.H. Goh, Single piles in lateral spreads: Field bending moment evaluation, J Geotech Geoenviron, 129 (2003) 879-889.
[19] R. Bouc, Mathematical Model for Hysteresis, Acustica, 24 (1971) 16-&.
[20] Y.K. Wen, Method for Random Vibration of Hysteretic Systems, J Eng Mech Div-Asce, 102 (1976) 249-263.
[21] D. Badoni, N. Makris, Nonlinear response of single piles under lateral inertial and seismic loads, Soil Dyn Earthq Eng, 15 (1996) 29-43.
[22] S. Wang, B.L. Kutter, J.M. Chacko, D.W. Wilson, R.W. Boulanger, A. Abghari, Non-linear seismic soil-pile-structure interaction, Earthquake Spectra, 14 (1998) 377-396.
[23] N. Makris, G. Gazetas, Dynamic Pile Soil Pile Interaction .2. Lateral and Seismic Response, Earthquake Eng Struc, 21 (1992) 145-162.
[24] S. Iai, Y. Matsunaga, T. Kameoka, Strain space plasticity model for cyclic mobility, Soils Found, 32 (1992) 1-15.
[25] I. Towhata, K. Ishihara, Modeling soil behavior under principal axes rotation, in: Fifth International Conference on Numerical Methods in Geomechanics, 1985, pp. 523-530.
[26] L. Gonzalez, T. Abdoun, R. Dobry, Effect of Soil Permeability on Centrifuge Modeling of Pile Response to Lateral Spreading, J Geotech Geoenviron, 135 (2009) 62-73.
[27] Varun, D. Assimaki, A Nonlinear dynamic macroelement for soil-structure interaction analyses of pile-supported waterfront structures, Int J Numer Anal Met, Submitted (2010).
[28] R. Popescu, J.H. Prevost, Comparison between Velacs Numerical Class-a Predictions and Centrifuge Experimental Soil Test-Results, Soil Dyn Earthq Eng, 14 (1995) 79-92.
[29] K. Arulanandan, R.F. Scott, Verification of numerical procedures for the analysis of soil liquefaction problems, in: International Conference on the Verification of Numerical Procedures for the Analysis of Soil Liquefaction Problems, A. A. Balkema, 1994.
[30] D.W. Wilson, Soil pile superstructure interaction in liquefying sand and soft clay, in, University of California Davis, 1998.